Quantum localization of coherent pi-electron angular momentum in (P)-2,2'-biphenol

ARTICLE · JANUARY 2014

READS
41

1 AUTHOR:

Hiroki Nakamura
National Chiao Tung University
238 PUBLICATIONS **4,129** CITATIONS

SEE PROFILE

THE JOURNAL OF PHYSICAL CHEMISTRY Letters

Letter

pubs.acs.org/JPCL

Quantum Localization of Coherent π-Electron Angular Momentum in (*P*)-2,2′-Biphenol

Masahiro Yamaki,[†] Hirobumi Mineo,[‡] Yoshiaki Teranishi,[§,∥] Michitoshi Hayashi,[⊥] Yuichi Fujimura,*[,†,‡,#] Hiroki Nakamura,[†] and Sheng Hsien Lin[†,‡]

[†]Institute of Molecular Science, Department of Applied Chemistry, National Chiao Tung University, Hsinchu, Taiwan 300, Republic of China

[‡]Institute of Atomic and Molecular Sciences, Academia Sinica, Taipei, Taiwan 106, Republic of China

[§]Institute of Physics, National Chiao Tung University, Hsinchu, Taiwan 300, Republic of China

[∥]Physics Division, National Center for Theoretical Sciences, Hsinchu, Taiwan 300, Republic of China

[⊥]Center for Condensed Matter Science, National Taiwan University, Taipei, Taiwan 106, Republic of China

[#]Department of Chemistry, Graduate School of Science, Tohoku University, Sendai, 980-8578 Japan

Supporting Information

ABSTRACT: Controlling π-electrons with delocalized character is one of the fundamental issues in femtosecond and attosecond chemistry. Localization of π-electron rotation by using laser pulses is expected to play an essential role in nanoscience. The π-electron rotation created at a selected aromatic ring of a single molecule induces a local intense electromagnetic field, which is a new type of ultrafast optical control functioning. We propose a quantum localization of coherent π-electron angular momentum in (*P*)-2,2′-biphenol, which is a simple, covalently linked chiral aromatic ring chain molecule. The localization considered here consists of sequential two steps: the first step is to localize the π-electron angular momentum at a selected ring of the two benzene rings, and the other is to maintain the localization. Optimal control theory was used for obtaining the optimized electric fields of linearly polarized laser pulses to realize the localization. The optimal electric fields and the resultant coherent electronic dynamics are analyzed.

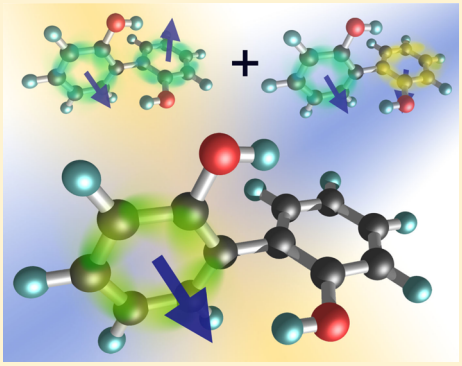

SECTION: Spectroscopy, Photochemistry, and Excited States

The π-electrons in aromatic molecules play a central role in chemistry.[1] They are the origin of various valence isomers formed by supplying heat or light.[2−4] This is due to their delocalized character. Mobile π-electrons have attracted considerable attention in the field of organic optoelectronics for ultrafast switching devices.[5,6] In nanoscale devices, once π-electron motion is realized at a localized site and then a site-selective ring current is generated, the localized current may be transferred from one site to another site by applying laser pulses, that is, transferred ring current, and then an ultrafast switching function is operative at a selected local site of a nanoscale molecule. The site-selective ring current generation and transferred ring current can generate an induced magnetic field, namely an ultrafast moving magnetic field. Research on electronic dynamics in molecular systems has been accelerated by recent developments of both laser technology[7−11] and electronic wavepacket theory.[12−16] Results of several theoretical studies on the generation and control of π-electron motions in aromatic ring molecules by ultrashort UV laser pulses have been reported.[17] Manz's group has shown by quantum chemical simulations that π-electrons in doubly degenerated excited states of Mg porphyrin can be rotated along the aromatic ring by resonant excitation by using femtosecond circularly polarized UV laser pulses.[18−20] The direction of the π-electron rotation, clockwise or anticlockwise, depends on the right- or left-circularly polarized pulse. Kanno et al. have shown that transient (coherent) ring currents of chiral aromatic molecules having no electronic angular momentum state, such as pyrazinophanes, can be created by coherent excitation of a pair of quasi-degenerate electronic excited states.[21−24]

Mineo et al. have proposed a laser-control scenario for creation of multidimensional ring currents in a nonplanar chiral aromatic molecule with two benzene rings, (*P*)-2,2′-biphenol, by using ultrashort linearly polarized UV laser pulses.[25,26] They noted that the π-electrons can be rotated along the two benzene rings, i.e., *L*- and *R*-ring (see Figure 1), with a definite phase and four patterns of the π-electron rotations are generated by using a linearly polarized UV laser pulse. They are denoted by [CC], [AA], [CA], and [AC], where capital

Received: April 9, 2014
Accepted: May 20, 2014
Published: May 20, 2014

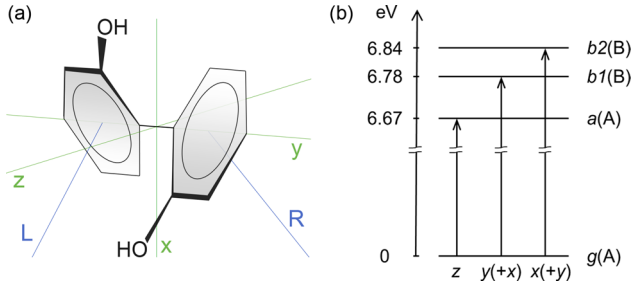

Figure 1. (a) Geometrical structure of (*P*)-2,2′-biphenol. (b) Electronic states adopted for quantum localization of π-electron rotations. *x*, *y*, and *z* specify directions of the electronic transition moments. (+*X*) means the *X*-component is minor (see text).

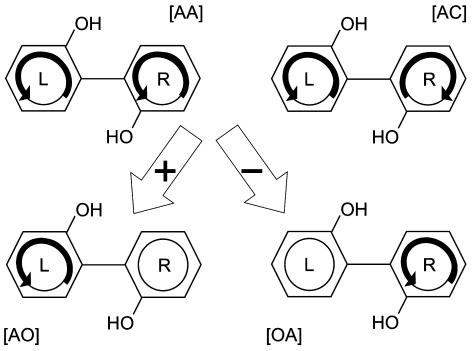

Figure 2. Superposition of coherent π-electron rotation patterns for quantum localization of π-electron at one of the rings. The arrow with positive (negative) sign specifies an in-phase (out-of-phase) superposition of [AA] and [AC] rotation patterns. The in-phase superposition creates [AO] rotation pattern, which means anticlockwise rotation localized on the *L*-ring with no rotation on the R-ring, while the out-of-phase superposition creates [OA] rotation pattern.

letters C and A refer to clockwise and anticlockwise rotations, respectively. The first and the last letter in bracket specify the rotational direction along the *L*- and *R*-ring, respectively. These four current patterns are coherently delocalized over the two rings connected. This result invokes a new interest. Whether π-electron angular momentum can be localized at a selected aromatic ring is one of the key issues in π-electron dynamics in a single molecule with covalently linked aromatic rings since it means that a strong ring current and a current-induced magnetic field can be generated at the selected aromatic ring, which may act as an active site.

In this paper, we propose a scenario of quantum localization of π-electron rotation along an aromatic ring of a single molecule with covalently linked chiral aromatic rings, and also show that it is possible to keep current localization as long as possible. A set of ultrashort linearly polarized UV pulsed lasers realizes quantum localization. The simplest real molecular model of a covalently linked chiral aromatic chain molecule, (*P*)-2,2′-biphenol, was adopted for quantum localization simulations. It is assumed to be fixed on the surface by a (CH_2) chain free from π-electrons. The geometrical structure of (*P*)-2,2′-biphenol (C_2 point group) is shown in Figure 1a. which was estimated by DFT calculations.[26,27] The rotation axis of the C_2 point group is placed along the laboratory-fixed *z*-axis parallel to the surface normal. The laboratory-fixed *y*-axis coincides with the covalent bond bridging the two phenol groups. The two benzene rings are twisted by 108.8°. The benzene ring in the negative region of the *y*-axis is called *L*-ring, and the other benzene ring in the positive region is called *R*-ring. In a similar way, the rotation axis of π-electrons perpendicular to the *L*-ring is called *L*-axis, and that perpendicular to the *R*-ring is called *R*-axis. The zenith angle is $\theta_K = 54.4°$ for $K = L,R$.

Localization of π-electron angular momentum can be intuitively understood from the four patterns of coherent π-electron rotations. Each pattern is generated by rotations of π-electrons localized at the two benzene rings with a definite rotational phase. Therefore, a linear combination of these patterns also gives other patterns of coherent electron motion, that is, localized or asymmetric rotational patterns. Figure 2 shows that a linear combination of [AA] and [AC] with in-phase, for example, generates an anticlockwise rotation of π-electrons along the *L*-axis, which results in the localization of π-electrons on the *L*-ring. This is referred to [AO]. Here, O means no rotation along the *R*-ring. Similarly, a linear combination of [AA] and [AC] with out-of-phase generates quantum localization of [OA]. In a previous study, we demonstrated that each rotational pattern can be created by a coherent excitation of a pair of nearly degenerated electronic states a (A), b_1 (B) and b_2 (B) whose energies range from 6.67 to 6.84 eV estimated by DFT calculation as shown in Figure 1b.[25] Here, excited state a belongs to the totally symmetric irreducible representation A in the C_2 point group, and excited states b_1 and b_2 belong to the antisymmetric irreducible representation B. These excited states originate from optically allowed quasi-degenerate excited states of the two phenol groups. Directions of the electronic transition moments are also shown by *x*, *y*, and *z* in Figure 1b. These three excited states, which constitute the minimum basis set, were used for describing quantum localization. Three types of linearly polarized UV pulses were used for carrying out coherent excitations. Transition moments from the ground state to these states are, $\boldsymbol{\mu}_{ag} = (0,0,-1.95)$, $\boldsymbol{\mu}_{b_1g} = (0.20, 4.92, 0)$, and $\boldsymbol{\mu}_{b_2g} = (3.14, -0.87, 0)$ in units of Debye. Since the primary purpose of present work is to demonstrate the possibility of localization and maintenance of π-electron rotations, both environmental perturbations and temperature effects are not considered.

It should be noted that the target state undergoes field-free time evolution just after the localization. For a practical purpose, it is important to keep the angular momentum localization of π-electrons as long as possible after the localization. Consideration should be given to quantum control to maintain the direction of the localized angular momentum generated. This means that actual control of the localization consists of sequential two steps: the first step is to localize the angular momentum at a selected ring, and the other is to maintain the direction of the angular momentum generated.

We apply optimal control theory[28,29] to the two steps. Quantum dynamics of π-electrons induced by the electric field of a laser pulse, $\mathbf{E}(t)$ is described by the Hamiltonian

$$\hat{H}(t) = \hat{H}_\pi - \hat{\boldsymbol{\mu}}\cdot\mathbf{E}(t) \quad (1)$$

Here, $\hat{H}_\pi$ is the π-electronic Hamiltonian of (*P*)-2,2′-biphenol in the free field and $\hat{\boldsymbol{\mu}}$ is the dipole moment operator. For simplicity, effects of molecular vibrations on electron dynamics are omitted.[34] Let us consider an objective functional,

dx.doi.org/10.1021/jz5007109 | J. Phys. Chem. Lett. 2014, 5, 2044−2049

$$J[\mathbf{E}] = \beta\langle\psi(T)|\hat{O}|\psi(T)\rangle + \frac{1-\beta}{T}\int_0^T dt\langle\psi(t)|\hat{O}|\psi(t)\rangle - \int_0^T dt\frac{\mathbf{E}(t)^2}{\hbar\alpha(t)} \quad (2)$$

which is to be maximized with a constraint of the time-dependent Schrödinger equation,

$$i\hbar\frac{\partial}{\partial t}|\psi(t)\rangle = \hat{H}(t)|\psi(t)\rangle \quad (3)$$

with the initial condition

$$|\psi(0)\rangle = |g\rangle \quad (4)$$

Here, $\hat{O}$ is a projection operator of target states, T is the control time, $\alpha(t)$ is a time-dependent penalty factor to suppress the intensity of the optimal field, β (= 0, 1) is a parameter to switch the objective functionals, and $|g\rangle$ is the ground state. In the case of $\beta = 1$, the population of target state is maximized at the final time. In the case of $\beta = 0$, on the other hand, the time-integrated population of target state is maximized. Taking the variation condition, $\delta J = 0$, the optimal electric field is obtained as

$$\mathbf{E}(t) = -\alpha(t)\mathrm{Im}\langle\xi(t)|\hat{\boldsymbol{\mu}}|\psi(t)\rangle \quad (5)$$

where $\xi(t)$ is the Lagrange multiplier that satisfies a time-dependent equation,

$$\left(i\hbar\frac{\partial}{\partial t} - \hat{H}(t)\right)|\xi(t)\rangle = (\beta - 1)\frac{i\hbar}{T}\hat{O}|\psi(t)\rangle \quad (6)$$

with the condition at the final time T,[28,29]

$$|\xi(T)\rangle = \beta\hat{O}|\psi(T)\rangle \quad (7)$$

In order to carry out quantum control simulation for localization of the π-electron angular momentum of (*P*)-2,2′-biphenol, we need a set of angular momentum eigenstates defined in each aromatic ring. Localization of the π-electron angular momentum can be intuitively explained by four patterns of electron rotations, which are constructed by three excited states (ϕ_a, ϕ_{b1}, ϕ_{b2}) as shown in Figure 1b. The localized angular momentum eigenstates (χ_K^A, χ_K^C with $K = L,R$) can be expressed in terms of the three excited states (ϕ_a, ϕ_{b1}, ϕ_{b2}) as

$$\begin{pmatrix}\chi_L^A\\ \chi_L^C\end{pmatrix} = \begin{pmatrix}0.56 & 0.71i & -0.43\\ 0.56 & -0.71i & -0.43\end{pmatrix}\begin{pmatrix}\phi_a\\ \phi_{b1}\\ \phi_{b2}\end{pmatrix} \quad (8a)$$

$$\begin{pmatrix}\chi_R^A\\ \chi_R^C\end{pmatrix} = \begin{pmatrix}-0.56 & 0.71i & -0.43\\ -0.56 & -0.71i & -0.43\end{pmatrix}\begin{pmatrix}\phi_a\\ \phi_{b1}\\ \phi_{b2}\end{pmatrix} \quad (8b)$$

The transformation matrices in eqs 8 are calculated by using the electronic angular momentum operator. See Supporting Information for a brief derivation of the transformation matrices. These states are the candidates for the target states of the optimal control. $\hat{O} = |\chi_L^A\rangle\langle\chi_L^A|$ for the [AO] localization, and $\hat{O} = |\chi_R^A\rangle\langle\chi_R^A|$ for the [OA] localization, for instance.

Let us first consider the quantum control of localization of π-electron rotations (first step). Here, we chose two cases for the localization. The first one is to localize the angular momentum with anticlockwise rotation around the *L*-axis, [AO], where the expectation values of the angular momenta around the *L*- and *R*-axes are given as $l_L(T) > 0$ and $l_R(T) = 0$, respectively. The other is to localize the angular momentum with anticlockwise rotation around the *R*-axis, [OA], that is $l_L(T) = 0$ and $l_R(T) > 0$. Figure 3 shows the results of quantum control for those cases, where we took $\beta = 1$ to obtain the target states at the final time. The parameter α of the time dependent penalty function $\alpha(t) = \alpha f(t)$ was chosen to be $\alpha = 33$ GV m^{-1} so as to obtain moderate electric field amplitude to suppress undesired multiphoton processes. Here, an envelope function, $f(t) = e^{-(t-0.01T)^2/(0.005T)^2}$ $(0 < t < 0.01T)$, $f(t) = 1$ $(0.01T < t < 0.99T)$, and $f(t) = e^{-(t-0.99T)^2/(0.005T)^2}$ $(0.99T < t < T)$ was employed to avoid sudden change of field amplitude. The control time, T = 30 fs, was chosen from inverse of the energy differences between two electronic excited states.

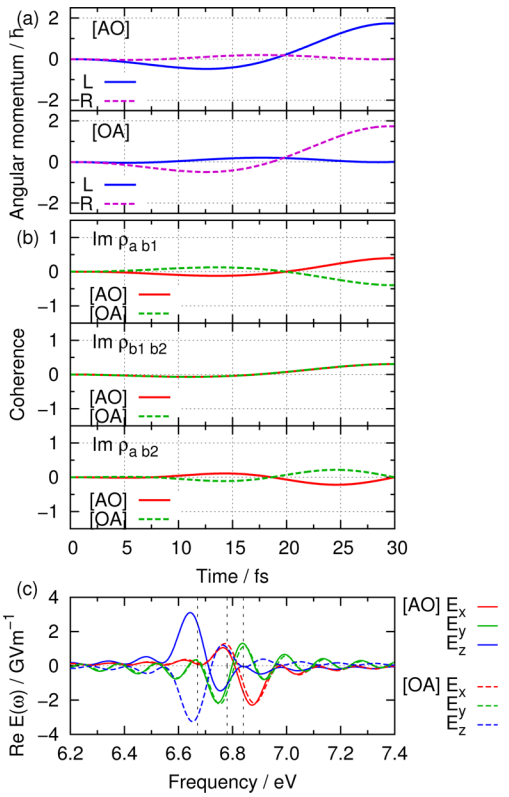

Figure 3. Results of quantum localization of π-electron rotations for the target [AO] and for the target [OA]. (a) Calculated time-dependent π-electron angular momenta $l_L(t)$ (blue solid line) and $l_R(t)$ (purple dashed line). (b) Imaginary parts of electronic coherences, $\rho_{b1a}(t)$, $\rho_{b2a}(t)$, and $\rho_{b1b2}(t)$. (c) Real parts of the optimal electric field in the frequency domain, $E_x(\omega)$, $E_y(\omega)$, and $E_z(\omega)$. Results of the [AO] ([OA]) target are shown in solid (dashed) lines. The phase of $E_z(\omega)$ is shifted by π between the two control targets.

Figure 3a represents the time-dependent expectation values of angular momenta around the *L*- and *R*-axes, $l_L(t)$ with blue solid line and $l_R(t)$ with purple dashed line. It can be seen that the expectation value at the target time, $l_L(T)$ ($l_R(T)$), reaches the maximum value for the [AO] ([OA]) target, while that of $l_R(T)$ ($l_L(T)$) is suppressed to zero. This indicates that the π-electron localization exclusively on one benzene ring is

dx.doi.org/10.1021/jz5007109 | J. Phys. Chem. Lett. 2014, 5, 2044−2049

successfully achieved. Figure 3b represents the results of coherent electronic dynamics driven by the optimal laser pulses. Only the imaginary parts of $\rho_{ab1}(t)$, $\rho_{b1b2}(t)$, and $\rho_{ab2}(t)$ are shown because the expectation value of angular momentum is proportional to the imaginary part of the electronic coherences.[25] The result for the [AO] target is shown in red solid line, and that for the [OA] target is shown in green broken line. It can be seen that $\rho_{b1b2}(t)$ for the [AO] and [OA] targets behave the same, while phases of $\rho_{ab1}(t)$ and $\rho_{ab2}(t)$ for the [AO] target are shifted by π compared to those for the [OA] target. These behaviors can be explained by comparing coefficients of the target states, χ_L^A and χ_R^A, shown in eqs 8. A product of coefficients of ϕ_a and ϕ_{b1} for χ_L^A gives a positive imaginary number, while that for χ_R^A is a negative one. As a result, $\rho_{ab1}(T)$ for [AO] and [OA] have opposite signs. Similarly, coefficients of ϕ_{b1} and ϕ_{b2} have the same sign for χ_L^A and χ_R^A, which results in the same sign of $\rho_{b1b2}(T)$. Coefficients of ϕ_a and ϕ_{b2} are real numbers so that $\rho_{ab2}(T)$ does not contribute to the angular momentum.

Figure 3c shows real parts of the optimal electric fields in the frequency domain, Re $\mathbf{E}(\omega)$, both for the [AO] target (solid line) and the [OA] target (dashed line). The vertical dotted lines indicate positions of the eigenstates (Figure 1b). The peaks of $E_x(\omega)$, $E_y(\omega)$, and $E_z(\omega)$ appeared at the resonant positions of b_2, b_1, and a states, respectively. It is clearly seen that the phases of the z-component are shifted by π between [AO] and [OA] targets, while phase shifts for the other two components, $E_x(\omega)$ and $E_y(\omega)$, are zero. This indicates that the π-phase shift of the electric field $E_z(\omega)$ is the key to control the π-electron rotations for the [AO] and [OA] localization. It should be noted that $E_z(\omega)$ excites only the a state as shown in Figure 1b. The only difference in the target coefficients in χ_L^A and χ_R^A is that of ϕ_a as shown in eqs 8. This is the reason why the π-phase shift appeared only in z-component. This phase shift of $E_z(\omega)$ results in π-phase shift in cofficients of ϕ_a, ϕ_{b1}, and ϕ_{b2}, and finally the [AO] and [OA] localization are realized at t = 30 fs. The maximum amplitude of the optimal field is about 1 GV m^{-1} (0.13 TW cm^{-2}), which is much lower than the so-called threshold of multiphoton processes.[30] The pulse shapes of $\mathbf{E}(t)$ are shown in the Supporting Information.

Let us next consider quantum control of the second step for the localization, that is to maintain the unidirectional (anticlockwise or clockwise) rotation of π-electrons around the L-axis, for instance. After the localization has been completed, the localized angular momentum spontaneously undergoes free propagation. Figure 4a shows the time dependence of the expectation values of the π-electron angular momentum under the field-free condition after the [AO] localization is achieved. Here, the initial time, t = 0 means the time when the localization has been completed in the first step. The expectation value of the π-electron angular momentum around the L-axis, $l_L(t)$ starts to oscillate, and that of around the R-axis, $l_R(t)$ deviates from zero and oscillates in the opposite way. It may seem that these oscillations of angular momenta continue with large amplitudes. They will dissipate away, however, since all energy eigenstates contribute to the angular momentum eigenstates in the real system, while our model only includes three excited states.

Figure 4b shows the results of the second step control to the initial localization demonstrated in Figure 3a. The parameter β = 0 is used to maximize the time integrated target states, which is similar to tracking problems in the quantum control of

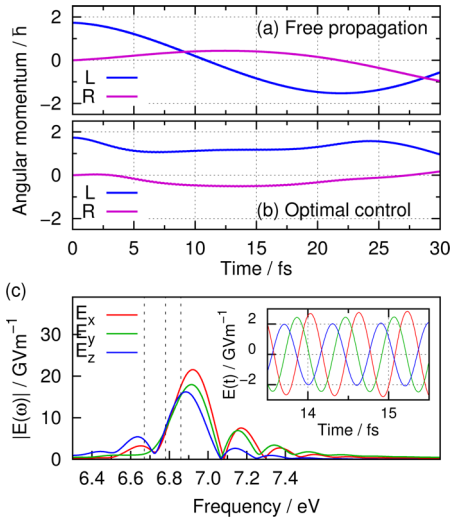

Figure 4. (a) Expectation values of π-electron angular momentum for the free rotations after the [AO] localization. (b) Results of the optimal control for maintaining the localization. The control time is T = 30 fs. (c) Absolute values of the optimal electric field in the frequency domain. The inset figure is the field in the restricted time domain.

chemical reaction.[29,31] The control time was again set at T = 30 fs, and α = 67 GV m^{-1} was used. The result shows that $l_L(t)$ keeps positive values under the optimal field, which means the direction of π-electron rotation is kept. Similar results can be obtained at any longer T > 30 fs. Although there exists small deviation, $l_R(t)$ is kept at around zero. The time-averaged expectation value of the target states, $J_L = \int_0^T \langle\psi(t)|\hat{O}|\psi(t)\rangle\, dt/T$, attained in the optimal control propagation is calculated to be 0.85, while that of the free propagation is 0.22. The amplitude of the optimal field is about 3 GV m^{-1} (1.2 TW cm^{-2}). Optimal control with larger α can give the better control, but such stronger field may cause multiphoton processes.

Figure 4c shows absolute values of the optimal electric fields in the frequency domain, E_x in red, E_y in green, and E_z in blue lines, respectively. The main peaks of all components appear at around 6.9 eV just above the highest eigenstates, b_2. The optimal field in the time domain $\mathbf{E}(t)$ is also shown in the inserted figure to indicate the phase relations. Compared to $E_x(t)$, $E_z(t)$ is shifted by π, and $E_y(t)$ is shifted by $\pi/2$, and these relations are almost kept during the control time. This means the resultant optimal field has an elliptically polarized character. Kanno et al. reported laser-polarization effects on coherent excitation of quasi-degenerate electronic states in chiral molecules with a single aromatic ring.[24] A possible mechanism of angular momentum transfer between the elliptically polarized electric field and (*P*)-2,2′-biphenol with two benzene rings may be analyzed by extending their treatment. The results of the detailed analysis on maintaining the electronic angular momentum by optimal control will be presented elsewhere.

Magnitudes of ring currents and those of current-induced magnetic fields can be evaluated from those of the corresponding angular momenta: the order of the ring currents is 100 μA, and that of the current-induced magnetic field measured at the center of the benzene ring is 100 mT.[26] We now just mention how to observe the localization of π-electron rotations around one of the benzene ring. This may be carried out by separately measuring the ring currents and magnetic

dx.doi.org/10.1021/jz5007109 | J. Phys. Chem. Lett. 2014, 5, 2044−2049

fields generated on the two phenol groups since the two benzene rings are not planar but tilted with the dihedral angle of 108.8° as shown in Figure 1.

The present simulations were performed using a simplified model of a closed system of single molecule for π-electron rotations in the low temperature limit. Here, "closed" system means that all influences originated from π-electron interactions with intramolecular vibrational modes, and heat bath modes were omitted. Mineo et al. recently found that intramolecular vibrational effects make significant contributions to dephasing of π-electron rotations under finite temperature conditions even in an isolated condition[32] as well as bath mode effects in condensed phases.[33] It has been also shown that nonadiabatic transitions strongly influence π-electron rotations in an isolated chiral aromatic molecules.[34] Application of optimal control theory to such open systems is one of the important subsequent issues. Basically, the control procedure in the Liouville space formalism should be adopted.[35,36]

In conclusion, we have proposed a quantum localization of π-electron angular momentum of (*P*)-2,2′-biphenol by using an optimal control procedure. By analyzing the results of optimization, we clarified the mechanisms of the localization and the mechanisms for maintaining the localization. This result suggests a possibility that the present current localization control is applicable to large molecular systems having covalently linked many benzene rings. Requirement for localization of π-electron rotations is to create a coherent superposition of quasi-degenerate excited states with angular momentum character. Creation of the electronic coherence is probed by observation of quantum beats in time-resolved spectra. For example, quantum beats in two-dimensional electronic spectra have been observed in excitation transfer in photosynthetic systems[37,38] and coherent intrachain energy migration in conjugated organic polymers at room temperature.[39] These experimental findings strongly suggest that localization of coherent π-electron rotations may be realized in a large-scale system even in condensed phases. Localization in a larger molecular system in which aromatic rings are covalently linked would be next interest.

Generation of a ring current at a selected aromatic ring is opposite to delocalization of π-electrons. Localization of π-electrons versus their delocalization is not only a fundamental issue in chemistry but may also play an important role in nanoscience. In addition, it is important to retain the localized angular momentum with a definite value as long as at least a vibrational period of a ring by restricting the phase change at the site created initially. Otherwise, delocalization of π-electrons occurs soon after the localization is completed. The principle proposed in this paper may be applicable, for instance, to maintain valence isomers of benzene, which are transiently produced by attosecond UV coherent pulses.[3]

■ ASSOCIATED CONTENT

Supporting Information

The matrix elements of the electronic angular momentum operator calculated from atomic orbital basis sets, and the optimal electric fields in the time domain $\mathbf{E}(t)$ for Figure 3c. This material is available free of charge via the Internet at http://pubs.acs.org.

■ AUTHOR INFORMATION

Corresponding Author

*E-mail: fujimurayuichi@m.tohoku.ac.jp.

Notes

The authors declare no competing financial interest.

■ ACKNOWLEDGMENTS

Y.F. thanks JSPS (Research Grant 23550003) and the National Science Council of Taiwan for financial support. H.M. thanks the National Science Council of Taiwan (Research Grant 102-2112-M-001-003-MY3) for financial support.

■ REFERENCES

(1) Minkin, V. L.; Glukhovtsev, M. N.; Simkin, B. Y. *Aromaticity and Antiaromaticity: Electronic and Structural Aspects*; John Wiley & Sons: New York, 1994.

(2) Houk, K. N.; Gonzalez, J.; Li, Y. Pericyclic Reaction Transition States: Passions and Punctilios, 1935−1995. *Acc. Chem. Res.* **1995**, *28*, 81−90.

(3) Ulusoy, I.; Nest, M. Correlated Electron Dynamics: How Aromaticity Can Be Controlled. *J. Am. Chem. Soc.* **2011**, *133*, 20230−20236.

(4) Moore, K.; Rabitz, H. Laser Control: Manipulating Molecules. *Nat. Chem.* **2012**, *4*, 72−73.

(5) Anthony, J. E. Functionalized Acenes and Heteroacenes for Organic Electronics. *Chem. Rev.* **2006**, *106*, 5028−5048.

(6) Bonifas, A. D.; McGreery, R. L. 'Soft' Au, Pt and Cu Contacts for Molecular Junctions Through Surface-Diffusion-Mediated Deposition. *Nat. Nanotechnol.* **2010**, *5*, 612−617.

(7) Mei, J. J.; Schafmeister, C.; Bird, G.; Paul, A.; Naaman, R.; Waldeck, D. H. Molecular Chirality and Charge Transfer through Self-Assembled Scaffold Monolayers. *J. Phys. Chem. B* **2006**, *110*, 1301−1308.

(8) Goulielmakis, E.; Loh, Z.-H.; Wirth, A.; Santra, R.; Rohringer, N.; Yakovlev, V. S.; Zherebtsov, S.; Pfeifer, T.; Azzeer, A. M.; Kling, M. F.; et al. Real-Time Observation of Valence Electron Motion. *Nature* **2010**, *466*, 739−743.

(9) Assion, A.; Baumert, T.; Bergt, M.; Brixner, T.; Kiefer, B.; Seyfried, V.; Strehle, M.; Gerber, G. Control of Chemical Reactions by Feedback-Optimized Phase-Shaped Femtosecond Laser Pulses. *Science* **1998**, *282*, 919−922.

(10) Chen, S.; Gilbertson, S.; Wang, H.; Chini, M.; Zhao, K.; Khan, S. D.; Wu, Y.; Chang, Z. Attosecond Pulse Generation, Characterization and Application. In: *Advances in Multi-photon Processes and Spectroscopy*; World Scientific: Singapore, 2011; Vol. *20*, Chapter 4.

(11) Yudin, G. L.; Bandrauk, A. D.; Corkum, P. B. Chirped Attosecond Photoelectron Spectroscopy. *Phys. Rev. Lett.* **2006**, *96*, 063002.

(12) Bandrauk, A. D.; Chelkowski, S.; Nguyen, H. S. Attosecond Localization of Electrons in Molecules. *Int. J. Quant. Chem.* **2004**, *100*, 834−844.

(13) Krause, P.; Klamroth, T.; Saalfrank, P. Time-Dependent Configuration-Interaction Calculations of Laser-Pulse-Driven Many-Electron Dynamics: Controlled Dipole Switching in Lithium Cyanide. *J. Chem. Phys.* **2005**, *123*, 074105.

(14) Král, P.; Seideman, T. Current-Induced Rotation of Helical Molecular Wires. *J. Chem. Phys.* **2005**, *123*, 184702.

(15) Remacle, F.; Levine, R. D. Attosecond Pumping of Nonstationary Electronic States of LiH: Charge Shake-up and Electron Density Distortion. *Phys. Rev. A* **2011**, *83*, 013411.

(16) Yuan, K.-J.; Bandrauk, A. D. Circularly Polarized Attosecond Pulses from Molecular High-Order Harmonic generation by Ultrashort Intense Bichromatic Circularly and Linearly Polarized Laser Pulses. *J. Phys. B: At. Mol. Opt. Phys.* **2012**, *45*, 074001.

(17) Fujimura, Y.; Sakai, H. Electron Rotation Induced by Laser Pulses. In *Electronic and Nuclear Dynamics in Molecular Systems*; World Scientific: Singapore, 2011; Chapter 6.

(18) Barth, I.; Manz, J.; Shigeta, Y.; Yagi, K. Unidirectional Electronic Ring Current Driven by a Few Cycle Circularly Polarized Laser Pulse: Quantum Model Simulations for Mg-Porphyrin. *J. Am. Chem. Soc.* **2006**, *128*, 7043−7049.

(19) (a) Barth, I.; Manz, J. Anregung Periodischer Elektronen-Kreisbewegung Durch Circular Polarisierte Laserpulse: Quantenmechanische Modell-Simulationen für Mg-Porphyrin. *Angew. Chem.* **2006**, *118*, 3028−3031;(b) Periodic Electron Circulation Induced by Circularly Polarized Laser Pulses: Quantum Model Simulations for Mg Porphyrin. *Angew. Chem., Int. Ed.* **2006**, *45*, 2962−2965.
(20) Barth, I.; Manz, J. Quantum Switching of Magnetic Fields by Circularly Polarized Re-Optimized π Laser Pulses: From One-Electron Atomic Ions to Molecules. In *Progress in Ultrafast Intense Laser Science VI*; Springer Series in Chemical Physics; Springer: Heidelberg, 2010; Chapter 2.
(21) Kanno, M.; Kono, H.; Fujimura, Y. Control of π-Electron Rotation in Chiral Aromatic Molecules by Nonhelical Laser Pulses. *Angew. Chem., Int. Ed.* **2006**, *45*, 7995−7998.
(22) Kanno, M.; Hoki, K.; Kono, H.; Fujimura, Y. Quantum Optimal Control of Electron Ring Currents in Chiral Aromatic Molecules. *J. Chem. Phys.* **2007**, *127*, 204314.
(23) Kanno, M.; Kono, H.; Fujimura, Y. Control of π-Electron Rotations in Chiral Aromatic Molecules Using Intense Laser Pulses. In *Progress in Ultrafast Intense Laser Science VII*; Springer: Heidelberg, 2011, Chapter 3.
(24) Kanno, M.; Ono, Y.; Kono, H.; Fujimura, Y. Laser-Polarization Effects on Coherent Vibronic Excitation of Molecules with Quasi-Degenerate Electronic States. *J. Phys. Chem. A* **2012**, *116*, 11260−11272.
(25) Mineo, H.; Yamaki, M.; Teranishi, Y.; Hayashi, M.; Lin, S. H.; Fujimura, Y. Quantum Switching of π-Electron Rotations in a Nonplanar Chiral Molecule by Using Linearly Polarized UV Laser Pulses. *J. Am. Chem. Soc.* **2012**, *134*, 14279−14282.
(26) Mineo, H.; Lin, S. H.; Fujimura, Y. Coherent π-Electron Dynamics of (*P*)-2,2′-Biphenol Induced by Ultrashort Linearly Polarized UV Pulses: Angular Momentum and Ring Current. *J. Chem. Phys.* **2013**, *138*, 674304.
(27) Frisch, M. J.; Trucks, G. W.; Schlegel, H. B.; Scuseria, G. E.; Robb, M. A.; Cheeseman, J. R.; Scalmani, G.; Barone, V.; Mennucci, B.; Petersson, G. A. et al. *Gaussian 09*, revision E.01; Gaussian, Inc.: Wallingford, CT, 2009.
(28) Zhu, W.; Botina, J.; Rabitz, H. Rapidly Convergent Iteration Methods for Quantum Optimal Control of Population. *J. Chem. Phys.* **1998**, *108*, 1953−1963.
(29) Serban, I.; Werschnik, J.; Gross, E. K. U. Optimal Control of Time-Dependent Targets. *Phys. Rev. A* **2005**, *71*, 053810.
(30) Bandrauk, A. D. *Molecules in Laser Fields*; Marcel Dekker: New York, 1994.
(31) Umeda, H.; Fujimura, Y. Quantum Control of Chemical Reaction Dynamics in a Classical Way. *J. Chem. Phys.* **2000**, *113*, 3510−3518.
(32) Mineo, H.; Lin, S. H.; Fujimura, Y. Vibrational Effects on UV/Vis Laser-Driven π-Electron Ring Currents in Aromatic Ring Molecules. *Chem. Phys.* **2014**, http://dx.doi.org/10.1016/j.chemphys.2014.02.011.
(33) Mineo, H.; Lin, S. H.; Fujimura, Y.; Xu, J.; Xu, R. X.; Yang, Y. J. Non-Markovian Response of Ultrafast Coherent Electronic Ring Currents in Chiral Aromatic Molecules in a Condensed Phase. *J. Chem. Phys.* **2013**, *139*, 214306.
(34) Kanno, M.; Kono, H.; Fujimura, Y.; Lin, S. H. Nonadiabatic Response Model of Laser-Induced Ultrafast π-Electron Rotations in Chiral Aromatic Molecules. *Phys. Rev. Lett.* **2010**, *104*, 108302.
(35) Sugawara, M.; Fujimura, Y. Control of Quantum Dynamics by Locally Optimized Laser Field. II. Application to a System with Dissipation. *J. Chem. Phys.* **1994**, *101*, 6586−6592.
(36) Ohtsuki, Y.; Zhu, W.; Rabitz, H. Monotonically Convergent Algorithm for Quantum Optimal Control with Dissipation. *J. Chem. Phys.* **1999**, *110*, 9825−9832.
(37) Engel, G. S.; Calhoun, T. R.; Read, E. L.; Ahn, T. K.; Mancal, T.; Cheng, Y.-C.; Blankenship, R. E.; Fleming, G. R. Evidence for Wavelike Energy Transfer through Quantum Coherence in Photosynthetic Systems. *Nature* **2007**, *446*, 782−786.
(38) Chung, Y.-C.; Fleming, G. R. Dynamics of Light Harvesting in Photosynthesis. *Annu. Rev. Phys. Chem.* **2009**, *60*, 241−262.
(39) Collini, E.; Scholes, G. D. Coherent Intrachain Energy Migration in a Conjugated Polymer at Room Temperature. *Science* **2009**, *323*, 369−373.